

# Seismic Response of Segmented Tunnel Liner

Hager A. Mitkees, Tamer M. Sorour, Mohammed A. Abdel-Motaa

**Abstract**— The use of tunnels has expanded in recent years to facilitate traffic, so dependable assessment of the seismic response of tunnel structures is critical in civil and earthquake engineering. Although tunnels are supported by segmental concrete linings, their behavior under the effect of joints is still ambiguous. Previous researches studied the seismic performance of tunnels assuming they are continuous conduit. They didn't consider the segmental effect, which would lead to variation in obtained results such as internal forces, tunnels liner deformation and consequently surrounding soil response. The purpose of this study is to investigate the segmental tunnels under seismic loads. The numerical tool used in this analysis is Plaxis 2D version 20.0.1.128 finite element software with Mohr-Coulomb material model. Results show that, existing of joints in tunnels makes tunnel more flexible and as a result of that, the settlement values increase and max bending moment in tunnel lining decreases with great values for the same lining thickness to diameter ratio. On the other hand, existing of joints has a low effect on normal forces values.

**Index Terms**—Finite element method, Mohr-Coulomb Model, Segmental Tunnel, Seismic Response.

## 1. INTRODUCTION

BEFORE the 1940s tunnel lining systems were characterized by bolting of steel plates through the flanges, but in the late twentieth century, the technology of pre-cast concrete tunnel lining segments appeared. Recently, tunnels are constructed using tunnel boring machine (TBM) machines, where it is used for successively boring underground, while pre-cast segments are simultaneously installed, and permanent tunnel liner formed. Each tunnel ring is completed by attaching number of pre-cast segments, which usually consists of 4 to 10 segments, depending on the tunnel geometry and other factors.

This study aims to examine the segmental effect of tunnel lining of its seismic response using equivalent linear model. Numerical analysis will be carried out using 2D finite element model. An initial comparison will be carried out to investigate the difference between previous work using sophisticated non-linear model and the proposed equivalent linear model. Parametric study will be carried out to examine the segmental effect of tunnel lining on the developed internal forces, tunnel deformation and the associated ground surface seismic response.

## 2. LITERATURE

Mohammed Ahmed Abdel-Motaa, Structural Department, Faculty of Engineering, Ain Shams University, Cairo, Egypt. Email: [abdelmotal@yahoo.com](mailto:abdelmotal@yahoo.com) [5] performed a comparison between pseudo static method, simplified dynamic analyses and full dynamic analyses in studying circular tunnels in transverse and longitudinal direction. For analytical analysis, equations by [19] had been used. Full dynamic analysis was done using 2-D finite element program (Plaxis) to model soil structure interaction. Earthquake was defined as acceleration time history at the base of model with peak acceleration 0.35g. [7]

• Hager Abd El Aziz Mitkees\*, Structural Department, Faculty of Engineering, Ain Shams University, Cairo, Egypt. Email: [Hager.Mitkees@eng.asu.edu.eg](mailto:Hager.Mitkees@eng.asu.edu.eg)

• Tamer Mohammed Sorour, Structural Department, Faculty of Engineering, Ain Shams University, Cairo, Egypt. Email: [tamer.sorour@eng.asu.edu.eg](mailto:tamer.sorour@eng.asu.edu.eg)

Mohammed Ahmed Abdel-Motaa, Structural Department, Faculty of Engineering, Ain Shams University, Cairo, Egypt. Email: [abdelmotal@yahoo.com](mailto:abdelmotal@yahoo.com)

studied the segmental lining tunnel using 2D plane strain model. The tunnel used in this study is Phase II Delhi Metro Line. Tunnels were studied under static and dynamic loads using different methods to apply dynamic loads. The tunnel was constructed using (TBM). The tunnel is 5.8 m diameter located at depth of 17.5m from ground surface. The tunnel consists of five segments and keystone. Two-dimensional (2D) plane strain model with Plaxis program were used where tunnel was modeled as beam elements. Soil was modeled using Mohr coulomb model in drained condition. For dynamics analysis, two earthquakes with variable intensity were applied using real earthquake data from COSMOS virtual data center. Earthquake were applied at bottom of soil layer assuming layer thickness 70m. To identify the damping, absorbent boundaries were also specified at both sides of the model to absorb the increments of stresses on the boundaries caused by the dynamic loading that would otherwise be reflected inside the soil body. [18] evaluated the stability state of Jiroft water-transform tunnel under static and dynamic loads using analytical method. Tunnel depth from ground surface was 80m with 2m radius, surrounded by rock. [19] equations were used to calculate the applied forces on the tunnel due to earthquake axial force and bending moment on a tunnel section considering the interaction of the tunnel concrete lining and rock mass. Two assumptions were taken in consideration for calculation forces in tunnel lining full slip and non-slip. [6] performed comparison between an experimental centrifuge test for tunnel surrounded by sand under seismic load and results of five numerical models using five different programs from five different papers. Each numerical analysis performed using different numerical code and different constitutive material model. The centrifuge tests also offer a suitable opportunity calibration of numerical models. In centrifuge tests, a smaller model than real problem was carried out therefore, scaling laws apply. [1] investigated seismic analysis for tunnels surrounded by dry sand considering soil structure interaction between tunnel and surrounding soil. An advanced nonlinear analysis was conducted using finite element model to simulate the problem considering nonlinearity and hysteresis of the soil. Soil

elements was modeled using two-dimension plane-strain four node elements. Three generated earthquakes were defined as time history acceleration modeled at the bedrock surface. [8] represented numerical studies on segmented tunnel liner under seismic load. Two-dimensional finite difference element model was created with constitutive soil model. Full dynamic analysis represented by time acceleration history has been used with the recordings of Naghan Fars Earthquake, which correspond to a low seismic signal and a high seismic signal. Analysis was done using the FLAC software. Soil was modeled as an elastic-plastic medium. Circular tunnel was modeled as an elastic beam. [4] performed a dynamic analysis for Cairo metro tunnel, which is considered a national great project in Egypt. It connects between three governorates Cairo, Giza & Qalyubia. It was constructed using slurry shield TBM. Tunnel is circular with 0.4m liner thickness, 8.35m internal diameter and 9.15m external diameter. Full dynamic analysis was done on tunnel using finite element program (Plaxis) taking soil structure interaction into consideration. The model was 2-D plane-strain model using elastic-plastic model based on Mohr-Coulomb failure criterion for soil. The earthquake was modified as acceleration time history modeled at the base of the model. [10] studied circular tunnels using 3-D finite element model. Full dynamic analysis calibrated on experimental results of a centrifuge test on a tunnel model in a dense dry sand subjected to transverse dynamic load by [6]. The numerical study includes two cases of continuous tunnel lining and segmental tunnel lining and comparing results obtained from two cases under different signals considering excavation method before applying seismic load. Joints of tunnel were modeled in longitudinal and transverse direction. Numerical 3D model was created using Plaxis, where soil was modeled using Harding soil model. Plate elements were used to model tunnel segments of 6m diameter and 0.3 m thickness. Acceleration time history applied at the base of model extracted from the European strong motion database that recorded during the South Iceland Earthquake, 2000 (M=6.6). [15] developed a numerical 3-D model using finite element method software MIDAS GTS NX in order to highlight the effect of the tunnel lining response under static and dynamic loads. The analysis was done on two twin tunnels with horizontal distance between the two tunnels centerline equal three times tunnel diameter. Construction stages were taken into consideration for static analysis. Earthquake was applied using modified response spectrum of UBC (1997) with damping ratio = 0.05. Tunnel was modeled in soft rock. The study show that the applied dynamic stress cannot be neglected for underground structure, but it is less dangerous in comparison with the superstructure.

Several different methods were used in literature for represents joints in tunnel lining. [1245] reduced the moment of inertia of the tunnel lining assuming that tunnels with joints are more flexible than continuous one. [13] assumed that segmental tunnel lining connected through elastic springs using analytical method. This method was developed to examine the effects of joint stiffness, joint distribution and

number. [11] studied the influence of the joint number, joint orientation, lateral earth pressure factor, and tunnel depth on the bending moment induced in a 6 m diameter segmental tunnel lining, using a finite element analysis program. In their analyses, the segmental joints were assumed to be fully hinged. [7] modeled joints in tunnels with full hinges in Plaxis using 2-D plane strain model. Results of bending moment of tunnel obtained zero moment at location of hinges. [21] conducted a numerical analysis using finite element program to represent the joint rotational stiffness, joint number, their distribution and the ground subgrade modulus on the bending moment. However, the interaction between the ground and the tunnel lining was considered only regarding a set of normal subgrade reaction springs, and not tangential ones. [8] Simulate joints in tunnel lining in 3D model using double nodes, which include six degrees of freedom. They are represented by three translational springs in the x, y and z directions, and three rotational springs around the x, y and z directions. Each spring can be defined by different stiffness value. For axial spring, it has been represented by a linear relation using a constant coefficient spring. The radial and rotational stiffness of a segment joint have been modelled by means of a bi-linear relation that is characterized by a stiffness factor and a maximum bearing capacity. [10] studied segmental tunnels using 3-D finite element model. Segments of tunnel were concrete volumes with elastic behavior. Longitudinal joints between tunnel segments were modeled as an elastic-perfectly plastic volumes with thickness = 0.30 m and width = 0.30 m, while transversal joints between the rings are modeled as interfaces with elastic-perfectly plastic behavior.

### 3. VERIFICATION OF THE NUMERICAL MODEL

Two case studies were performed to verify the model constructed by Plaxis 2D. First case study was performed on the tunnel soil system considering continuous tunnel lining. In the verification model, soil was modeled using Mohr Coulomb, an equivalent linear elastoplastic model to compare results with nonlinear soil model used by [1]. Results also compared with results estimated by analytical equations of [19]. Construction stages were taken into consideration in this case. Second case study was performed on a Contract BC-24 Phase II Delhi Metro Line, which is a segmental tunnel with five segments and keystone to study effect of static and seismic loads on the tunnel. Joints were modeled using hinges with free rotations. Construction stages were ignored in this case. Results were compared with results obtained by [7]. In the two cases, tunnel soil system was modeled using 2-D Plane strain model, using Plaxis 2-D program. Mohr coulomb model was used to simulate soil behavior. Soil elements modeled using 15 nodes triangle elements. Tunnel lining was modeled with plate elements, using linear elastic model to simulate concrete properties. Earthquake was applied at the bedrock surface as acceleration time history. For the first case study soil was a well graded dry sand. Four layers of sand soil with total thickness 30 m were defined to represent non linearity of soil

properties with depth given by [1] as shown in Fig. 1. Table I showing equivalent input soil properties for the four layers of sand soil, where their thicknesses were 3, 7, 10 and 10 m respectively. For tunnel lining the modulus of elasticity for concrete was taken  $2.4 \times 10^7$  Kpa and poisson's ratio  $\nu$  was 0.15. The source of dynamic excitation used in this verification model was the artificial acceleration-time history given by [2] and it was the same used by [1]. Fig. 2 shows the acceleration-time history of the record. For second case study a borehole was taken in area of tunnel showing five meters of fill followed by 65 m silty sand soil. Table II shows equivalent input soil properties for the two soil layers. The modulus of elasticity for tunnel lining was taken  $3.354 \times 10^7$  Kpa and poisson's ratio  $\nu$  was 0.15. Earthquake data was taken from Roorkee station which located about 150km away from Delhi. Roorkee Station also about 160km from Chamoli, of which was adopted as the reference earthquake source. Peak acceleration recorded at Roorkee Station is 0.55 m/s<sup>2</sup>. Fig. 3 shows acceleration time history for earthquake. For first case comparison was done between internal forces diagram on tunnel lining due to seismic load only between generated model and Literature values by [1] as shown in Fig. 4, Fig. 5 & Fig. 6. Results also were compared to values obtained by analytical expressions of [19]. There is a good agreement between the results of bending moment and shear forces distribution on tunnel lining under seismic loads of verification model, formulas by [19] and results in literature by [1]. On the other hand, results of FEM for normal force are average between [19] and results obtained by [1]. For second case study Fig. 7, Fig. 8 & Fig. 9 show the internal forces in segmental tunnel lining using finite element model (FEM) and results obtained by [7]. Referring to these figures, it is observed that: Results of the finite element model and results obtained by [7] are almost identical.

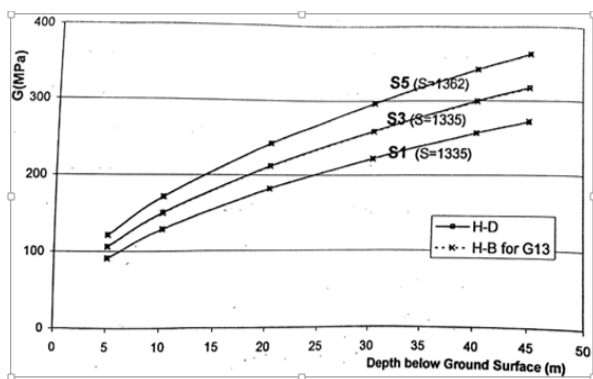


Fig. 1. Shear modulus variation with depth for types of soil used by [1]

Color					
$\gamma$	kN/m <sup>3</sup>	16.73	16.73	16.73	16.73
<b>e init</b>		0.554	0.554	0.554	0.554
<b>E</b>	kN/m <sup>2</sup>	2.8 E5	2.8.E5	4.0E5	5.0E5
<b>v (nu)</b>		0.3390	0.3390	0.3390	0.3390
<b>G</b>	kN/m <sup>2</sup>	104.6E3	104.6E3	156.8E3	186.7E3
<b>E oed</b>	kN/m <sup>2</sup>	429.3E3	429.3E3	643.9E3	766.5E3
<b>c ref</b>	kN/m <sup>2</sup>	6.000	1.000	1.000	1.000
<b><math>\phi</math> (phi)</b>	degree	30.00	30.00	30.00	30.00
<b>V s</b>	m/s	247.6	247.6	303.3	330.9
<b>V p</b>	m/s	<b>501.7</b>	<b>501.7</b>	<b>614.5</b>	<b>670.5</b>

Table II: Input soil properties for second verification model

Identification		Fill	Silty Sand
<b>Colour</b>			
$\gamma$	kN/m <sup>3</sup>	19	21
<b>e init</b>		0.5	0.5
<b>E</b>	kN/m <sup>2</sup>	1.30E6	1.30E6
<b>v (nu)</b>		0.3	0.3
<b>G</b>	kN/m <sup>2</sup>	500.0E3	500.0E3
<b>E oed</b>	kN/m <sup>2</sup>	1.75E6	1.75E6
<b>c ref</b>	kN/m <sup>2</sup>	2.5	2.5
<b><math>\phi</math> (phi)</b>	degree	28.00	30.00
<b>V s</b>	m/s	508.1	508.1
<b>V p</b>	m/s	950.6	950.6

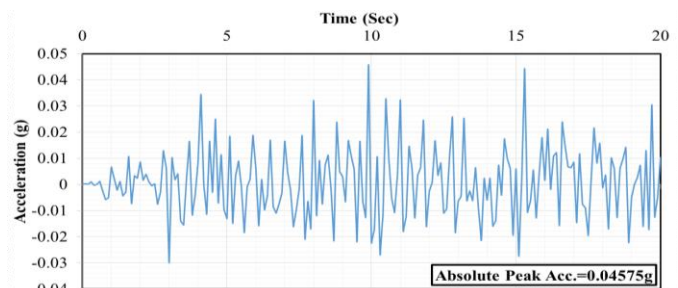


Fig. 2. Artificial acceleration-time history given by [2]

Table I: Input soil properties for first verification model

Identification	Units	1	2	3	4

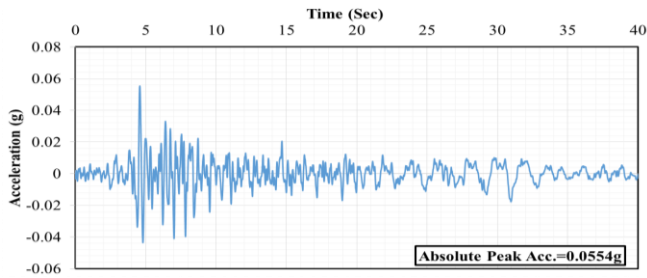


Fig. 3. Input acceleration time history from Rookree station

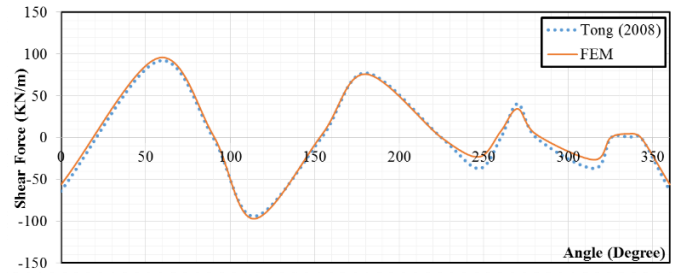


Fig. 8. Shear force diagram on tunnel lining

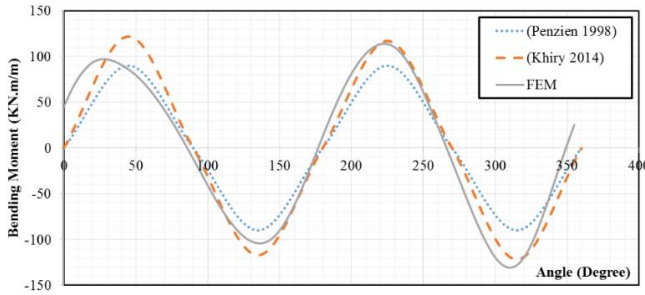


Fig. 4. Bending moment distribution on tunnel lining

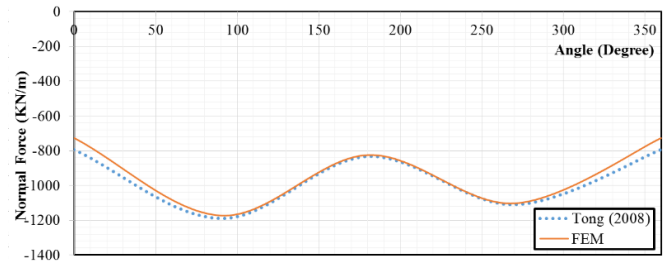


Fig. 9. Shear force diagram on tunnel lining

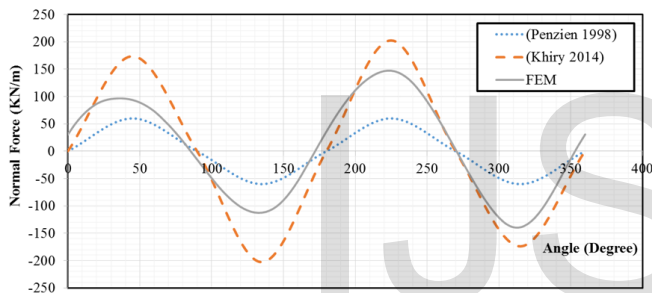


Fig. 5. Normal force distribution on tunnel lining

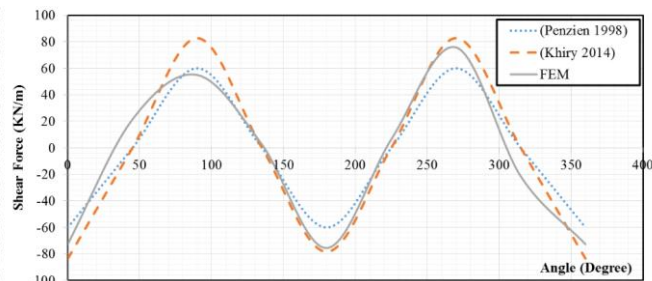


Fig. 6. Shear force diagram on tunnel lining

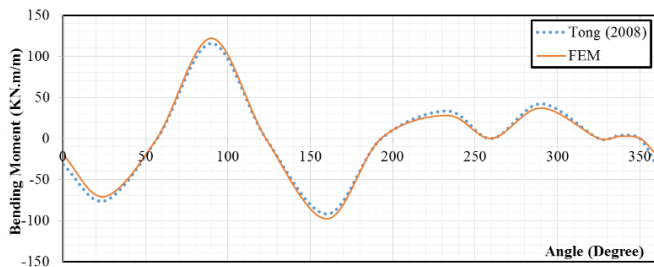


Fig. 7. Bending moment distribution on tunnel lining

## 4. NUMERICAL ANALYSIS FOR SEGMENTED TUNNEL

### 4.1 Model Descriptions

Analysis is done for segmental tunnel using 2-D finite element plain strain model. The soil layer thickness is taken 70m in all the following analysis. A dry dense sand is the type of soil used in the analysis. Soil is modeled using elastoplastic Mohr Coulomb model. All earthquake ground motions are applied at the bedrock surface in all dynamic analysis. Earthquake is applied using acceleration time history as input motion in direction perpendicular to tunnel axis. Tunnels are modeled using 2-D plate elements. Fig. 10 shows the 2-D plane strain model. The mesh density is set to be medium density in general, while density of mesh is increased at tunnel area to get more accurate results as shown in Fig. 11. Tunnels diameters are taken with values ranges between 6 to 12 m. Tunnel lining thickness is taken with values ranges between 0.3 to 0.9m. Depth of tunnel from ground surface is taken from 9m to 18m. Hinges with free rotation are used to simulate joints in tunnel lining. Number of joints taken in analysis ranges between zeros for continuous tunnel to 12 joints. For static analysis standard boundaries which is vertical and horizontal fixation for transition for bottom boundary and HZ fixation for vertical boundaries. For dynamic analysis, free field and compliant base boundaries are used to avoid reflection of waves into model, which lead to distortions in results. Four stages of construction are performed as follow:

First stage: Activate soil around tunnel hole to take its own weight into consideration, deactivate soil in the tunnel hole, and activate internal pressure  $P_i$ .

Second stage: Activate liner of the tunnel which is plate element so its own weight will be taken in analysis,  $P_i$  still with its initial value.

Third stage: Decreasing value of  $P_i$  gradually and finally it

turns to zero.

Fourth stage: Applying earthquake load.

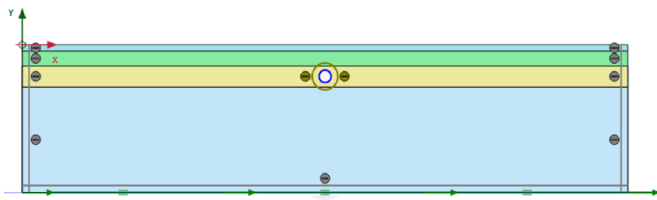


Fig. 10. 2-D plane strain model

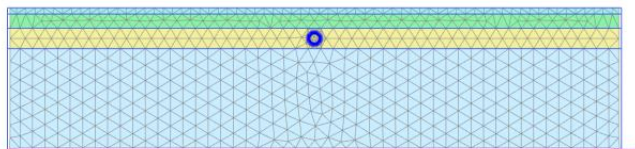


Fig. 11. (2-D) mesh

### 4.1 Soil Properties

In all analysis soil properties values are constant in all models. Soil used in this analysis are a well graded dry sand. Four layers of sand soil are defined to represent nonlinearity of soil properties with depth. Four successive soil layers are considered as shown in Fig. 10. Their thicknesses are 3, 7, 10 and 50 m respectively. Soil elements modeled using 15 nodes triangle elements as shown in Fig. 12. Table I showing equivalent input soil properties for the four layers of sand soil. As shown in Table 1 friction angle is taken constant with 30 degree, the dry unit weight for the four layers was taken constant with value equal 16.729 KN/m<sup>3</sup>. A very small value for cohesion of first layer of soil (C=6 KN/m<sup>2</sup>) is given to avoid mathematical complications due to the lack of shear strength of the surface layer. Soil cohesion for other layers is taken (C=1 KN/m<sup>2</sup>). Modulus of elasticity is increasing with depth as shown in Table I.

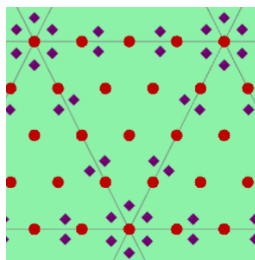


Fig. 12. The 15-nodes triangle soil element

### 4.1 Properties of Tunnel Lining

Properties of lining structure are considered constant during all analysis. The modulus of elasticity for concrete is taken 2.4x 10<sup>7</sup> Kpa and poisson's ratio (ν) 0.15. Tunnel lining is modeled with 2-D plate elements using linear elastic model. Table III shows entire tunnel lining properties in Plaxis.

Table III: Tunnel lining Properties

MATERIAL		

TYPE		ELASTIC
ISOTROPIC		Yes
EA 1	kN/m	1.20E+07
EA 2	kN/m	1.20E+07
EI	kN m <sup>2</sup> /m	2.50E+05
T	m	0.5
W	kN/m/m	25
N (NU)		0.15

### 4.1 Joints

Joints are modeled as hinges with free rotations. Number of joints used in the following analysis are four, six, eight, ten and twelve joints. The distribution of joints for all cases is symmetric. Fig. 13 shows the distribution of joints for each case.

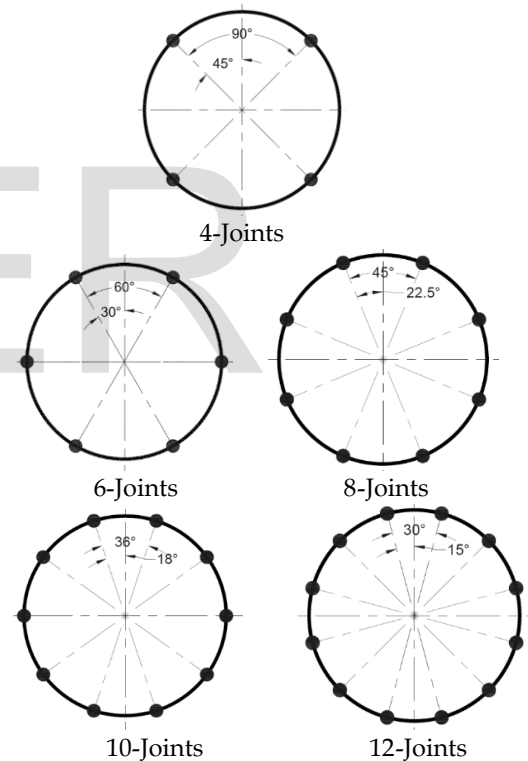


Fig. 13. Joints Distribution

### 4.1 Earthquake Time History

Earthquake used in the analysis is called Denali earthquake occurred in 2002 in Denali in North America. Data is recorded by Alaska (TAPS Pump Station #07) which located 203.5 Km away from Denali. Earthquake period recorded at this station is 60 sec. Earthquake data is taken from COSMOS Virtual Data Centre. Fig. 14 shows acceleration time history for the earthquake. Earthquake was scaled to 0.05g, 0.1g, 0.15g & 0.2g.

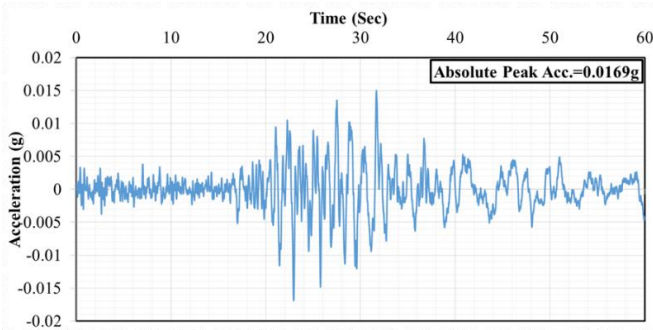


Fig. 14. Acceleration time history for Denali earthquake

#### 4.1 Numerical Results

Fig. 15 shows a relation between number of joints in tunnel cross section and the maximum bending moment for three ratios of lining thickness to diameter ( $t/D = 0.0375, 0.0625 \& 0.0875$ ) and tunnel depth 15m. The input base acceleration for these analyses is 0.15g. Referring to this figure, it is shown that the average percentage of decrease in bending moment for six joints tunnel is 44% comparing to continuous tunnel. Fig. 16 also shows a relation between number of joints in tunnel cross section and max normal force for the same earthquake intensity and same ratios of lining thickness to tunnel diameter. Fig. 17 shows relation between max normal force and number of joints is showed for only number of joints (0, 4, 8 & 12). For number of joints (0, 4, 8 & 12) by increasing number of joints max normal force in tunnel lining decreases with small values for the same lining thickness to diameter ratio. The average percentage of decrease in normal force for eight joints tunnel is 22% comparing with continuous tunnel. However, for 6&10 joints have different effect on values of normal force and thus is due to distribution of joints. As shown previously in Fig. 13 distribution of joints is symmetric in all directions for no. of joints (0, 4, 8 & 12), although for no of joints 6&10 distribution of joints is not symmetric in all directions.

In order to study the effect of changing ratio of lining thickness to tunnel diameter on bending moment on tunnel, a relation between ratio of lining thickness to diameter ( $t/D$ ) and bending moment was performed for max moment in tunnel. Fig. 18 shows relation between ratio ( $t/D$ ) and max bending moment for four earthquake intensities (0.05g, 0.1g, 0.15g and 0.2g), considering tunnel diameter 8m at 15m depth. Fig. 19 shows variation of max normal force in tunnel lining with lining thickness to diameter ratio for different earthquake intensity (0.05g, 0.1g, 0.15g and 0.2g).

Then with the aim of studying the effect of changing tunnel diameter on bending moment and compression force on tunnel, a relation between tunnel diameter and max bending moment was performed. Fig. 20 shows variation between tunnel diameter and bending moment for earthquake intensity (0.15g), variable lining thickness (0.3, 0.5, 0.7 & 0.9) and tunnel depth 15m. Fig. 21 shows variation of max compression force in tunnel lining with tunnel diameter for earthquake intensity (0.15g) and different lining thickness (0.3, 0.5, 0.7 & 0.9).

For studying the effect of changing tunnel depth on bending

moment and compression force in tunnel, a relation between tunnel depth and bending moment was plotted and a relation between max normal force in lining and tunnel depth also was performed. Fig. 22 shows variation between tunnel depth and max bending moment for different earthquake intensities (0.05g, 0.1g, 0.15g & 0.2g). Fig. 23 shows variation of max normal force in tunnel lining with tunnel depth for different earthquake intensities (0.05g, 0.1g, 0.15g & 0.2g).

For studying the effect of changing previous parameters on settlement trough, the following figures were plotted. Fig. 24 shows settlement trough due to seismic load for tunnel diameter 8m and lining thickness 0.5 m for different number of joints (0, 4, 6, 8, 10 & 12). As shown in this figure, by increasing number of joints in tunnel lining, tunnel becomes more flexible and as a result of that settlement values increases. The percentage of increase in settlement is 33% for 12 joints tunnel comparing to continuous one. The further we are from tunnel centerline, settlement trough for different number of joints becomes closer. Fig. 25 shows the effect of lining thickness to tunnel diameter ratio on settlement trough using four ratios (0.0375, 0.0625, 0.875 & 0.1125) for tunnel diameter 8m, tunnel depth 15m and constant number of joints (six joints). The effect of decreasing ratio of lining thickness to tunnel diameter has low effect on settlement trough values. The percentage of increase is 10% for ratio  $t/D$  (0.0375) comparing to ratio  $t/D$  (0.1125). Fig. 26 shows settlement trough under seismic load for different tunnel diameter (6, 8, 10 & 12) with constant lining thickness 0.5m, tunnel depth 15m and constant number of joints (six joints). It is obvious from previous figure that increasing tunnel diameter leads to increase values of settlement under seismic load. The increase extends for long distance from center line. The average percentage of increase is 59% for tunnel with diameter 12m comparing to 6m diameter. Fig. 27 shows the effect of tunnel depth on settlement trough using four depths (9, 12, 15 & 18) for tunnel diameter 8m, lining thickness 0.5, base acceleration 0.15g and constant number of joints (six joints). Increasing tunnel depth leads to increase values of settlement under seismic load. The increase extends for long distance from center line. The average percentage of increase is 71% for tunnel at depth 18m comparing to tunnel at depth 9m.

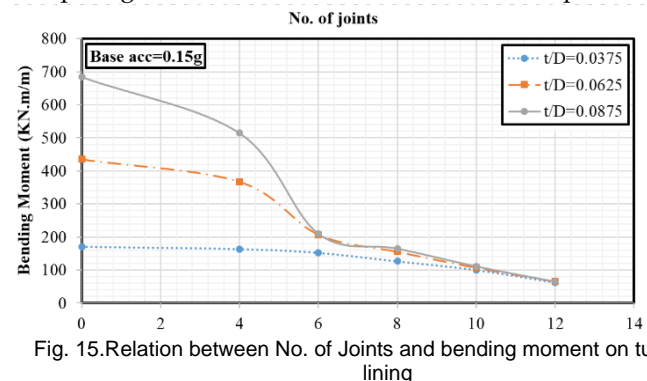


Fig. 15. Relation between No. of Joints and bending moment on tunnel lining

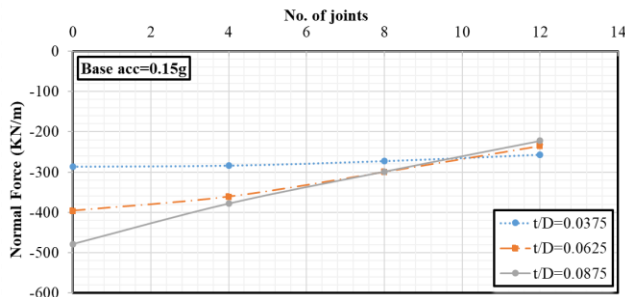


Fig. 16. Relation between No. of Joints and compression force on tunnel lining for (0, 4, 8 & 12) joints

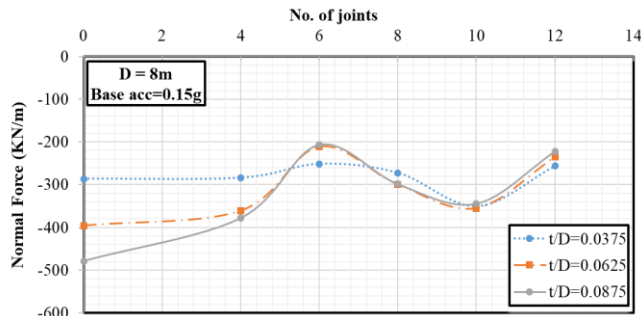


Fig. 17. Relation between No. of Joints and compression force on tunnel lining for (0, 4, 6, 8, 10 & 12) joints

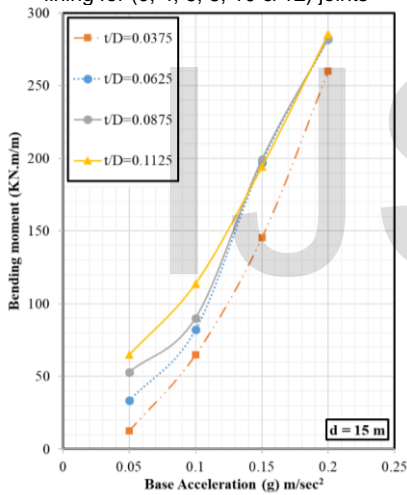


Fig. 18. Relation between Max bending moment considering different (t/D) ratios for variable earthquake intensity

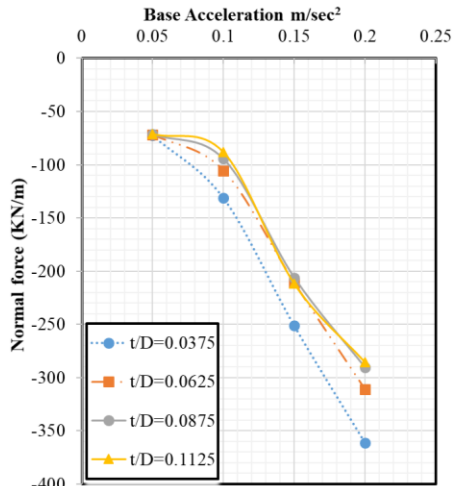


Fig. 19. Variation of max Normal force with (t/D) ratio for different earthquake intensity

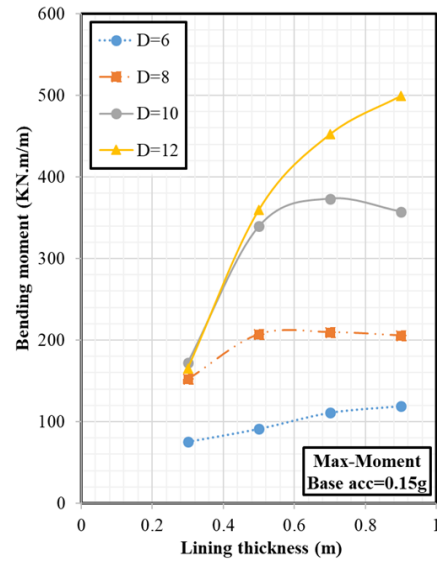


Fig. 20. Relation between tunnel diameter and Max bending moment for different lining thickness

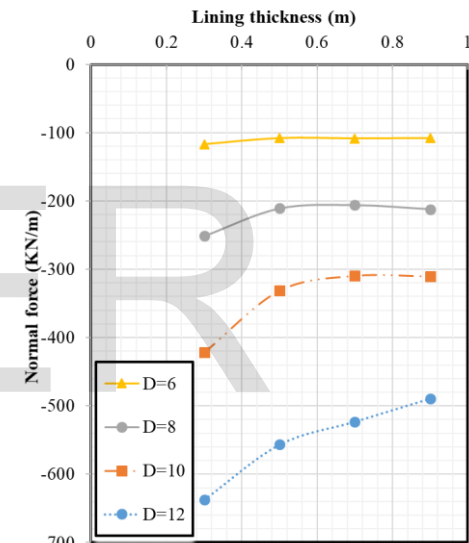


Fig. 21. Variation of normal force with tunnel diameter for diff. lining thickness

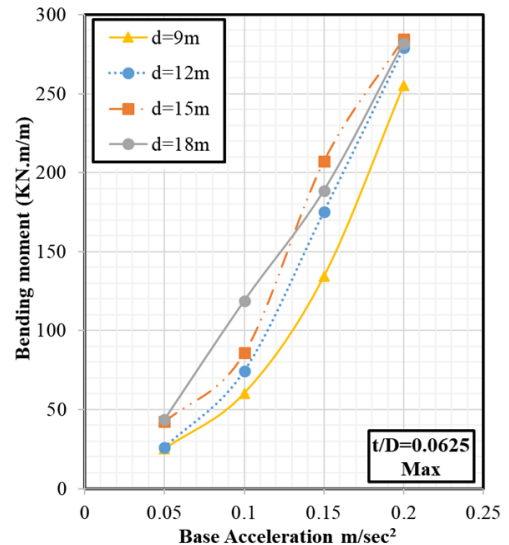


Fig. 22. Variation of max bending moment with tunnel depth for variable earthquake intensity

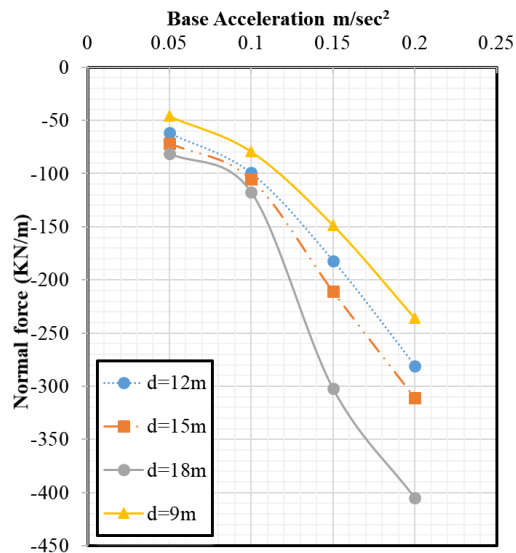


Fig. 23. Variation of max normal force with tunnel depth for variable earthquake intensity

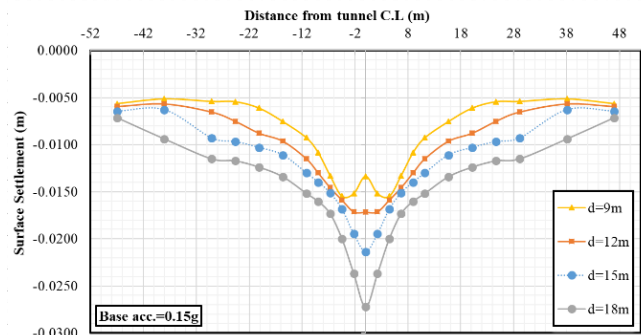


Fig. 27. Effect of Tunnel depth on settlement trough

### 5. CONCLUSION

The research findings summarize as follows:

- 1) Two-dimensional finite element modeling (2D FEM) using Plaxis program can accurately describe the behavior of the tunnel-soil system under static and seismic loads.
- 2) Applying the Mohr Coulomb model provides acceptable results comparing to results of nonlinear model.
- 3) Construction stages for tunnels using TBM must be taken into consideration to get actual values for straining actions in tunnel lining under static loads.
- 4) Changing the absolute peak acceleration at base affects the shape of the acceleration time histories. Peak values of acceleration at ground surface increase with increasing peak values at bedrock surface. The peak values of acceleration are magnified at shallower depths above the bedrock towards the ground surface.
- 5) Increasing earthquake intensity leads to increase in bending moment in tunnel liner for all points in tunnel lining, but the rate of increase is different from point to other.
- 6) Changing lining thickness to diameter ratio has a minor effect on the values of max bending moment and normal force in tunnel lining.
- 7) The location of maximum bending moment varies with variation of earthquake intensity.
- 8) Max normal force in tunnel increases with increasing earthquake intensity.
- 9) In general, increasing tunnel diameter leads to great increase in max bending moment and max normal force in tunnel lining for different lining thickness.
- 10) As a result of increasing number of joints in tunnel lining, max bending moment in tunnel lining decreases with great values for the same lining thickness to diameter ratio. The average percentage of decrease in bending moment for six joints tunnel is 44% comparing to continuous tunnel.
- 11) For low rigid tunnel, existing of joints has low effect on bending moment and normal force values comparing to highly rigid tunnel.
- 12) Existing of joints has a low effect on normal forces values, however distribution of joints has a clear effect on normal force values.
- 13) Study shows that for different ratios of lining thickness to diameter max compression force in tunnel lining is almost

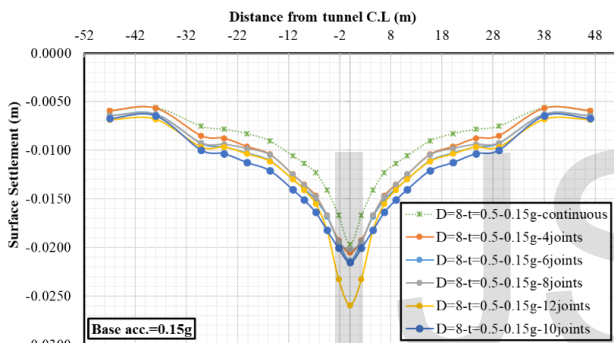


Fig. 24. Effect of number of joints on settlement trough

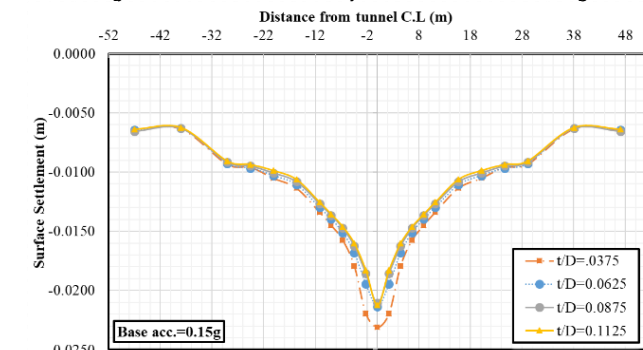


Fig. 25. Effect of Lining thickness to diameter ratio (t/D) on settlement trough

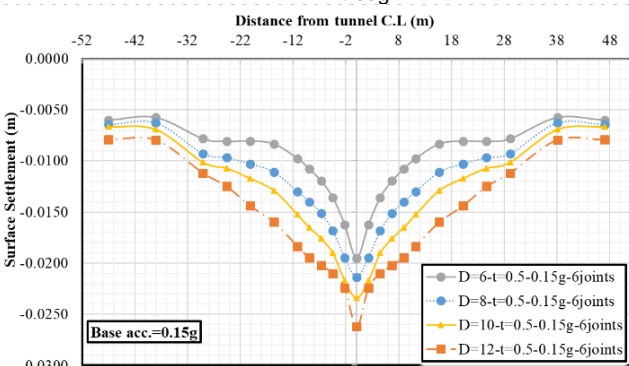


Fig. 26. Effect of tunnel diameter on settlement trough



same by increasing number of joints.

- 14) Changing tunnel depth has low effect on max bending moment values thus for high earthquake intensity, the average percent of increase is 25%, however for low earthquake intensity average percent of increase is 85%.
- 15) By increasing tunnel depth, max normal force in lining increases obviously for all earthquake intensities. The average percentage of increase in normal force is 75%.
- 16) Under seismic load, existing of joints leads to increase in flexibility of tunnel and as a result of that, the settlement trough values increase comparing to non-joints tunnel (continuous liner).
- 17) By increasing number of joints in tunnel lining, tunnel becomes more flexible and as a result, the settlement values increase.
- 18) It is obvious from previous figure that increasing tunnel diameter leads to increase values of settlement under seismic load. The increase extends for long distance from center line. The average percentage of increase is 59% for tunnel with diameter 12m comparing to 6m diameter.
- 19) The effect of decreasing ratio of lining thickness to tunnel diameter makes tunnel more flexible and as result of that settlement values increase but the increase is in the location of tunnel and for far distance settlement values are almost same. The percentage of increase is 10% for ratio  $t/D$  (0.0375) comparing to ratio  $t/D$  (0.1125).
- 20) Increasing tunnel depth leads to increase values of settlement under seismic load. The increase extends for long distance from center line. The average percentage of increase is 71% for tunnel at depth 18m comparing to tunnel at depth 9m.

## REFERENCES

- [1] Abdel-Motaa, M. A., El-Nahas, F. M., & Khiry, A. T. (2014). Mutual seismic interaction between tunnels and the surrounding granular soil. *HBRC Journal*, 10(3), 265-278. <https://doi.org/10.1016/j.hbrj.2013.12.006>
- [2] Abdel-Motaa, M. (1999). Soil effect on the dynamic behavior of framed structures (Doctoral dissertation, Ph. D. Thesis, Faculty of Engineering, University of Ain Shams, Cairo).
- [3] Abdel-Motaa, M., Khairy, A., & El-Nahas, F. (2006). Effect of tunnel presence on the change of the free field seismic response. *J Soil Mech. Found. Egypt. Geotech. Soc. i HBRC*, 17(1), 107-122.
- [4] Adam, M. A., Elleboudy, A. M., & Soliman, M. F. (2016). Seismic Site Response Analysis of a Cairo Metro Tunnel. In *Geotechnical and Structural Engineering Congress 2016* (pp. 1114-1126).
- [5] Bilotta, E., Lanzano, G., Russo, G., Santucci de Magistris, F., Aiello, V., Conte, E., ... & Valentino, M. (2007, June). Pseudostatic and dynamic analyses of tunnels in transversal and longitudinal directions. In *Proceedings of the 4th international conference on Earthquake Geotechnical Engineering*. Thessaloniki: Springer.
- [6] Bilotta, E., Lanzano, G., Madabhushi, S. P. G., & Silvestri, F. (2014). A numerical Round Robin on tunnels under seismic actions. *Acta Geotechnica*, 9(4), 563-579. <https://doi.org/10.1007/s11440-014-0330-3>
- [7] Chow, W. L., Tang, S. K., & Tong, S. Y. (2009). Design of segmental tunnel lining in an earthquake zone. In *ITA-AITES World Tunnel Congress*.
- [8] Do, N. A., Dias, D., & Oreste, P. (2014). 2D seismic numerical analysis of segmental tunnel lining behaviour. *Bulletin of the New Zealand Society for Earthquake Engineering*, 47(3), 206-216. <https://doi.org/10.5459/bnzsee.47.3.206-216>
- [9] Earthquake Data from COSMOS Virtual Data Centre.
- [10] Fabozzi, S., & Bilotta, E., (2017). Effect of flat joints on the seismic behaviour of a segmental tunnel lining.
- [11] Hefny, A., & Chua, H. (2006). An investigation into the behaviour of jointed tunnel lining. *Tunnelling and Underground Space Technology*, 21(3-4), 428. <https://doi.org/10.1016/j.tust.2005.12.070>
- [12] Khairy, A. (2006). Dynamic Response of Tunnels under Seismic Loads (Doctoral dissertation, Ph. D. Thesis, Faculty of Engineering, University of Ain Shams, Cairo).
- [13] Lee, K. M., Hou, X. Y., Ge, X. W., & Tang, Y. (2001). An analytical solution for a jointed shield-driven tunnel lining. *International Journal for Numerical and Analytical Methods in Geomechanics*, 25(4), 365-390. <https://doi.org/10.1002/nag.134>
- [14] Menkiti, C O, and R J Mair. 2001. Symposium Underground Construction. <https://www.researchgate.net/publication/331593874>.
- [15] Mohammed, J., & Hrubesova, E. (2018). Numerical modelling for twin horizontal circle tunnels under static and dynamic loads. *GCEC 2017*, 111-124. [https://doi.org/10.1007/978-981-10-8016-6\\_9](https://doi.org/10.1007/978-981-10-8016-6_9)
- [16] Muir Wood, A. M. (1976). Discussion: The circular tunnel in elastic ground. *Géotechnique*, 26(1), 231-237. <https://doi.org/10.1680/geot.1976.26.1.231>
- [17] Guidelines for the design of shield tunnel lining. (2000). *Tunnelling and Underground Space Technology*, 15(3), 303-331. [https://doi.org/10.1016/s0886-7798\(00\)00058-4](https://doi.org/10.1016/s0886-7798(00)00058-4)
- [18] Oraee, B., N. Hosseini, K. Oraee, and M. Gholinejad. 2011. "Analyses of Tunnel Stability under Dynamic Loads." *SME Annual Meeting and Exhibit and CMA 113th National Western Mining Conference 2011*: 781-84.
- [19] Penzien, J., & Wu, C. L. (1998). Stresses in linings of bored tunnels. *Earthquake Engineering & Structural Dynamics*, 27(3), 283-300. [https://doi.org/10.1002/\(sici\)1096-9845\(199803\)27:3<283:aid-eqe732>3.0.co;2-t](https://doi.org/10.1002/(sici)1096-9845(199803)27:3<283:aid-eqe732>3.0.co;2-t)
- [20] Plaxis 2D Connect edition V20 Tutorial Manual.
- [21] Teachavorasinskun, S., & Chub-uppakarn, T. (2010). Influence of segmental joints on tunnel lining. *Tunnelling and Underground Space Technology*, 25(4), 490-494. <https://doi.org/10.1016/j.tust.2010.02.003>
- [22] Wang, J.-N., 1993. *Seismic Design of Tunnels: A State-of-the-Art Approach*, Monograph, monograph 7, Parsons. Brinckerhoff Quade and Douglas Inc., New York.
- [23] Yu, H., Chen, J., Bobet, A., & Yuan, Y. (2016). Damage observation and assessment of the Longxi tunnel during the Wenchuan earthquake. *Tunnelling and Underground Space Technology*, 54, 102-116. <https://doi.org/10.1016/j.tust.2016.02.008>